Particle-velocity distribution and expansion of a surface-flashover plasma in the presence of magnetic fields

Y. Maron, E. Sarid, O. Zahavi, L. Perelmutter, and M. Sarfaty
Department of Physics, Weizmann Institute of Science, Rehovot, 76 100, Israel
(Received 27 January 1988; revised manuscript received 26 January 1989)

Observations of line-emission Doppler broadening and Doppler shift are used to determine the velocity distributions, parallel and perpendicular to the anode surface, of neutral particles and multiply charged ions in a surface-flashover-produced plasma in a magnetically insulated ion diode. The velocity distributions were found to be nearly Maxwellian with thermal energies of $\simeq 8$ eV for neutral particles, $\simeq 20$ eV for singly charged ions, and 20–80 eV for doubly and triply charged ions. The plasma-pressure gradient in the magnetic field, obtained from the observed ion temperature and density, and a suggested anomalous plasma conductivity that is approximately ten times lower than the classical conductivity are shown to explain the fast plasma expansion with respect to the magnetic field. Elastic collisions of the 7-eV electrons with the hotter ions cause electron heating. The observed ion velocities in the plasma parallel to the anode account for $\simeq \frac{1}{3}$ of the velocities in the same directions observed in the diode acceleration gap in a previous experiment.

I. INTRODUCTION

The behavior of plasmas in pulsed devices ($\lesssim 100$ ns) is strongly influenced by the ion and neutral-particle velocity distributions in the plasma. The ion kinetic energies affect the plasma pressure (and thus the plasma expansion), the electron-ion energy transfer due to elastic collisions, and, in the presence of magnetic fields in the plasma, the ion Larmor radii. The energies of neutral particles affect their motion and thus their densities and ionizations throughout the plasma. The ion and neutral-particle flows in the plasma determine the extraction of various ions from plasmas under electric fields.

In particular, the properties of plasmas formed over dielectric surfaces in pulsed high-voltage systems play an important role in the operation of the systems. For example, the expansion of the anode plasma in high-power ion diodes[1–3] causes time-dependent changes in the electric-field distribution, in the charge flow and in the impedance of the diode.

Little information on the mechanisms that dominate the anode-plasma expansion in pulsed diodes is presently available. Johnson and co-workers[4] used visible-light interferometry to observe the relatively dense part of the anode plasma ($\simeq 4\times 10^{16}$ cm^{-3}) in a 700-kV 300-kA 80-ns magnetically insulated ion diode (in such diodes magnetic field is applied parallel to the electrodes in order to inhibit the electron flow across the diode gap and thus to increase the ion-beam generation efficiency[5]). They observed an expansion velocity of about 1.5 cm/μs. Maenchen *et al.*,[6] also using interferometry, observed velocities of up to 30 cm/μs in axial plumes of the anode plasma in a pinch-reflex diode operating at 1.5 MA and 1.5 MV. In an applied B-ion diode (1.7 MV, 1.7 MA), Johnson *et al.*[7] have reported that an expansion velocity of 5 to 10 cm/μs throughout the voltage pulse was required for their surface-flashover anode plasma in order to explain the temporal impedance decrease. Pal and Hammer[8] determined the electron density from the H_β-line broadening in a lower power experiment (400 kV, 20 kA) using a planar magnetically insulated diode.[9] They showed plasma expansion velocities of 1–2 cm/μs. Recent measurements[10] of the electric-field distribution in the acceleration gap of planar diode configurations (300 kV, 20 kA) provided information about the expansion of the electric-field-excluding plasma. The plasma was seen to occupy about a 3-mm-wide region near the anode surface early in the pulse and to expand at $\simeq 1$ cm/μs later on in the pulse. These velocities of plasma expansion against the magnetic field are not explained as yet.

Generally, the ions in the anode plasma in high-power diodes were believed to be much colder than the electrons, based on the slow rate of the electron–heavy-particle energy transfer. The electron temperature was assumed[4] to be of a few electron volts. The observed[10] relatively fast expansion of the surface-flashover anode plasma in intense ion diodes raised the possibility that the ion kinetic energies in these plasmas are higher than commonly assumed.

To the best of our knowledge, until now the particle motion in plasmas produced in pulsed-power devices had been investigated by time-dependent measurements of spatial distributions[8,11] of optical emission lines. However, the particle excitation and ionization states undergo strong local temporal variations in such nonequilibrium plasmas. It may, therefore, be misleading to extract particle velocities from spatial line-intensity profiles, as shown in Ref. 12. Moreover, while such measurements may provide the average particle velocity they do not give the particle-velocity distribution.

In this study we report on the determination of ion and neutral-particle velocity distributions in a surface-flashover anode plasma in a planar magnetically insulated diode by the observation of the Doppler broadening of

the line emission of various particles. The measurements are performed as a function of time and distance from the anode surface, parallel and perpendicular to the surface. They yield the particle-velocity distributions directly, thus avoiding the difficulties discussed above.

Formation of the anode plasma via a surface flashover of a dielectric anode is widely used in intense ion-beam diodes.[13] Based on observed correlation of the ion-beam generation with the bombardment of the anode surface by electrons accelerated in the diode, Johnson and coworkers[14] suggested that electron leakage to the anode causes surface breakdown by generating electric fields with large tangential components on the dielectric surface. The anode plasma is then formed as a result of electric breakdown in neutral-particle desorbed gas released by electron impact of both primary and secondary electrons on the dielectric surface. The processes responsible for the plasma formation and the material release from the surface are not addressed in this study.

The velocity distributions parallel to the anode were observed both for particles originating from adsorbates on the dielectric surface and for particles contained in the dielectric material. For the latter, the particles were locally "seeded" in the dielectric, allowing investigations of geometrical effects and plasma uniformity. The velocity distributions parallel to the anode were found to be nearly Maxwellian. The kinetic energies of neutral particles and ions of various charge states were found to be about 8 eV and 20–80 eV, respectively, significantly higher than what has been commonly believed. The ions appeared to move away from the anode with a nearly isotropic (in half of the velocity space) velocity distribution. We have not as yet studied the processes responsible for the particle kinetic energies and for the observed temporal and spatial energy variations in the plasma.

Since the ions are hotter than the electrons [the electron temperature was determined to be $\simeq 7$ eV (Ref. 15)], electron-ion elastic collisions cause electron heating rather than electron cooling. Also, the relatively large ion kinetic energies cause a high plasma pressure, obtained using the electron density observed from the Stark and Doppler broadening of H_α and H_β lines, and thus a large plasma-pressure gradient. The latter enhances the plasma expansion against the magnetic field (the applied magnetic field was observed to be present in the plasma early in the pulse[16]). However, assuming classical electron conductivity,[17] the calculated rate of the plasma expansion away from the anode, based on the observed ion temperature and electron density, is still smaller than the rate observed. Also, the currents induced in the plasma by the electron flow in the diode acceleration gap are estimated to push the plasma back to the anode surface. We then suggest that the plasma conductivity is $\simeq 10\times$ lower than the classical conductivity. This should result in a significant reduction in the induced currents in the plasma and in a faster expansion of the plasma due to its pressure gradient, which is shown to explain the observed expansion rate. The plasma current due to the pressure gradient, together with the anomalous conductivity, also possibly dominate the electron heating in the plasma, as shown in Ref. 12.

A mechanism that may be responsible for the anomalous plasma conductivity is the lower-hybrid-drift instability in the low-drift-velocity regime.[18,19] The electron-drift velocity, obtained from the plasma-pressure gradient, is used to estimate the growth rate and the associated anomalous conductivity which are found to be reasonably close to the requirements.

The average ion velocity parallel to the magnetic-field lines in the anode plasma as observed in this work is about $\frac{1}{3}$ of the average ion velocity observed in a similar experiment[20] in the same direction in the diode acceleration gap. The ion velocities in the plasma parallel to the electrodes set a lower limit to the divergence of ion beams produced from surface-flashover plasma sources. However, if these velocities do not increase for higher diode voltages ($\gtrsim 10$ MV), this limit would be sufficiently small to allow beam applications in inertial-confinement pellet fusion.[3] The effects of the particle kinetic energies reported here on the particle flow, ionization of neutral particles, and ion extraction from the plasma, are discussed in detail in Ref. 12.

II. EXPERIMENTAL ARRANGEMENT

For the present experiments we used a planar magnetically insulated diode, shown in Fig. 1(a), similar to that described by Maenchen *et al.*[9] The insulating magnetic field B_z was produced by driving a 250-kA 30-μs current pulse through the cathode that acted as a single-turn coil. The magnetic field was varied in the experiments between 5 and 9 kG. Three-mm wide slots were cut in the y direction in the cathode to allow 50% ion transmission. An end view of the diode is shown in Fig. 1(b). A 14-cm-long thin stainless-steel vane was connected to the cathode, opposite the top of the active (dielectric) anode, parallel to the magnetic-field lines (electrons emitted from the vane $\mathbf{E}\times\mathbf{B}$ drifted in the diode gap downward). The anode-cathode gap and the distance between the anode and the vane tip were 8 and 5 mm, respectively.

The active anode [see Fig. 1(c)] was made of epoxy that filled grooves in an aluminum plate. The grooves were along the z direction, unless stated otherwise. The epoxy grooves and the separating aluminum ribs were 3.8 and 0.7 mm wide, respectively. The height in the y direction of the active anode h_y was 6 cm and its length in the z direction l_z was varied in the experiments between 2 to 14 cm.

The diode was powered by a 270-kV 90-ns pulse delivered by an LC generator coupled to a 1-Ω water line. The use of a low-impedance line was advantageous for our experiments since it allowed the voltage pulse height on the relatively high-impedance (usually >10 Ω) diode to be almost independent of the applied magnetic field and the active-anode area that were changed in the experiments. Typical diode voltage and current wave forms are shown in Fig. 2.

Light was collected from the anode plasma parallel to the magnetic-field lines (as shown in Fig. 3). Fused silica optics were used to direct the light to the spectrometer input slit through the demagnifying lens L. These mea-

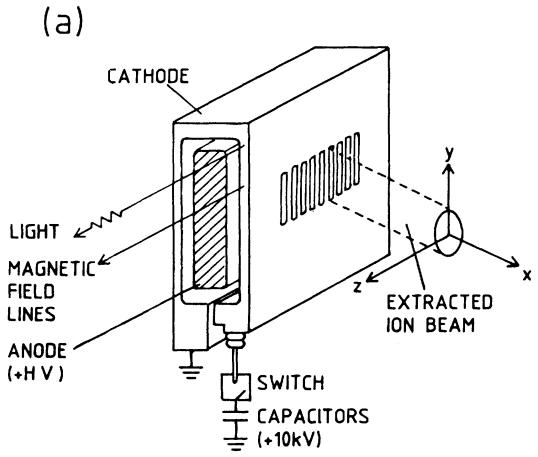

FIG. 1. (a) Schematic illustration of the planar magnetically insulated ion diode. HV denotes high voltage. (b) An end view of the diode showing the location of the cathode vane and the active anode region. (c) A view of the anode showing the active anode geometry. The active anode length and height are l_z and h_y, respectively. The shaded area shows an example of an anode part (of length l_s) in which the epoxy was mixed with the desired compound.

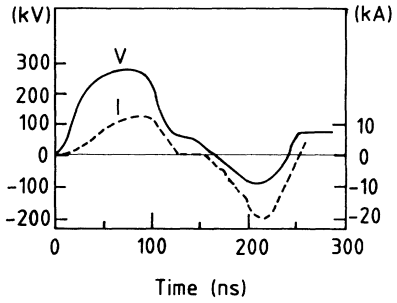

FIG. 2. Typical diode voltage (monitored by a capacitive probe) and current waveforms for $B_z = 7.0$ kG.

surements integrated along the active anode length. The spatial resolution in the x direction was determined by the spectrometer input-slit width, the demagnification of the lens L, and the anode length (due to defocusing along the line of sight). The spatial resolution was varied in the experiments between 0.3 and 0.9 mm by changing each of these parameters. In the measurements the system collected light only from the 3.5-cm-high central part of the anode, in order to exclude light from the cathode-vane plasma or from the plasma on the aluminum anode stalk.

In order to observe particle kinetic energies of a few electron volts from line Doppler broadening a spectral resolution of 0.1 Å is required. We used a 1-m spectrograph equipped with a 2400-groove/mm grating. Using the cylindrical lens CL, the image at the spectrograph output window was about ten times magnified, thus improving the reciprocal linear dispersion to 0.3 Å/mm. The light was then collected by a rectangular array made of nine quartz-fiber bundles, each 0.25-mm wide and 15-mm high. Each fiber bundle transmitted the light signal to a broadband photomultiplier tube. The spectral resolution thus obtained was $\lesssim 0.1$ Å. The photomultiplier-tube signals were recorded by oscilloscope-camera systems with a temporal resolution of about 5 ns. Thus, nine points on the spectral line profile were obtained in a single discharge. The nine spectral channels were calibrated with respect to each other over the entire usable spectrum. The distance x from the anode of the region

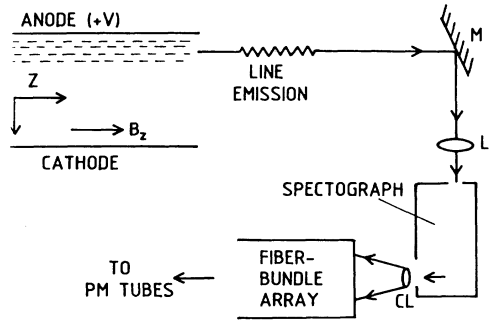

FIG. 3. Illustration of the optical arrangement. M, L, and CL are a mirror, a lens, and a cylindrical lens, respectively. The distance from the anode of the observed region is varied by moving the mirror M in the x direction.

viewed by the optical system was varied in the experiments by displacing the mirror M.

In order to allow velocity measurements for different species the epoxy used for the anode was mixed with powder of the desired-species compound (usually salt). This procedure also allowed us to obtain local measurements by seeding the epoxy with the observed species only in limited portions of the dielectric anode, with a length l_s, as shown in Fig. 1(c). Observing line emission from different parts of the plasma enabled us to check the plasma uniformity and to examine the influence of edge effects. This localization of the line emission was not possible for carbon and hydrogen which were produced over the entire area of the active anode. The particle-velocity distributions were found to be insensitive to the admixture used for the anode epoxy, as discussed in Sec. III.

III. MEASUREMENTS AND RESULTS

A. Axial line intensity distribution

Qualitative information about the plasma width in the axial direction can be obtained from measurements of ion line-emission intensities as a function of time and distance from the anode surface. An example is shown in Fig. 4, where axial intensity distributions of the C III 2297-Å line are shown for four time instants after the start of the diode voltage pulse. In these experiments $l_z = l_s = 2$ cm and the spatial resolution, due to the 20-μm-slit width and the defocusing along the 2-cm-long active anode, was $\lesssim 0.3$ mm.

In our measurements line emission from the plasma is seen to start rising at $t \simeq 20$ ns. At $t \simeq 55$ ns the plasma is seen to occupy a region about 1.5-mm wide near the anode surfaec (see Fig. 4). This gives a velocity of at least 3 cm/μs for the plasma expansion during this early stage of the pulse. Later on in the pulse the plasma appears to expand at about 1 cm/μs during which period the areal plasma density continuously increases, as shown in Sec. III D. This plasma motion is similar to that observed in recent experiments[10] using similar diode configurations and similar voltage and current pulses. In those experiments the plasma was observed to exclude the diode electric field from about a 3-mm-wide region at $t = 35$ ns and to expand later on in the pulse at about 1 cm/μs. This expansion rate during the later stage of the pulse is consistent with the observations of Pal and Hammer[8] obtained using a similar diode configuration. The early plasma formation and expansion will be further discussed in Sec. IVA. The measurements to be presented in this paper refer only to the period $t \gtrsim 20$ ns during which spontaneous line emission was observed.

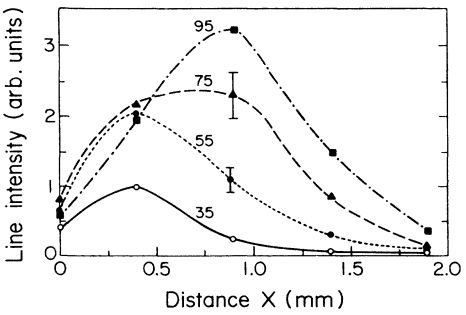

FIG. 4. Intensity of the C III 2297-Å line as a function of distance x from the anode surface for four times given in nanoseconds after the start of the diode voltage pulse. The lines are smooth curves that connect the data points. Here, $l_z = l_s = 2$ cm and the spatial resolution due to the spectrograph slit width (20 μm) and the defocusing along the anode is $\lesssim 0.3$ mm. The uncertainty is $\pm 15\%$, mainly due to shot-to-shot irreproducibility.

B. Particle-velocity distribution parallel to the anode surface

1. Selection of suitable lines

In order to obtain the particle-velocity distribution from an emission-line spectral profile, the profile must be dominated by Doppler broadening. To this end we selected lines that are very little broadened by encounters with plasma particles at the present plasma density (3×10^{15} cm^{-3}, see Sec. III D). Secondly, the Zeeman splitting due to the magnetic field in the plasma must be small with respect to the Doppler broadening. This requirement was satisfied in our measurements by using short-wavelength lines since the Zeeman splitting to Doppler broadening ratio decreases with wavelength. Thirdly, the mean free path for absorption must be large compared with the plasma length along the line of sight. This was verified for all the measurements reported here (see Sec. III B 7).

2. Velocity distributions of neutral and ionic carbon

A profile of the C III 2297-Å line observed in the z direction for a 4-cm-long active anode ($l_z = 4$ cm) is shown in Fig. 5(a). The indicated uncertainties resulted

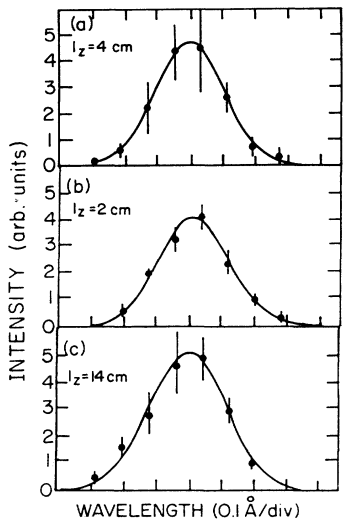

FIG. 5. Spectral profiles of the C III 2297-Å line observed in the z direction for active-anode lengths $l_z = 4$, 2, and 14 cm, shown in (a), (b), and (c), respectively. Here, $x = 1$ mm and $t = 85$ ns. Also shown are best-fit Gaussian curves.

from the uncertainty in the synchronization of the photomultiplier-tube traces (overestimated here to be ±5 ns) and from the uncertainty in the relative calibration of the fiber channels. The resulting error in determining the full width at half maximum (FWHM) of this line is estimated to be ±10% (for the wider lines the error is smaller). In addition, due to the uncertainty in the spectral width of each fiber channel, the absolute values of all velocities reported in this paper have a common uncertainty factor of ±6%. The reproducibility of the line profiles for different discharges was within 20%.

A best fit of a Gaussian curve to the data points, presented in Fig. 5(a), shows that such a curve fits the measured profile satisfactorily. Most of our measured profiles could be similarly fitted to Gaussian curves and this is assumed throughout this paper. The Gaussian fits to the data are corrected for the small contributions of the system spectral resolution, the Zeeman splitting in a parallel-to-B observation, and the Stark broadening. For the line in Fig. 5(a), the contributions of the latter two factors are 0.04 Å and <0.01 Å,[21,22] respectively. For brevity, we will henceforth not give the contributions of these two factors for each line separately, since they were small for all the lines reported here. The Stark broadening values were taken from Refs. 21–24. The corrected profiles define nearly Gaussian velocity distributions, proportional to $\exp(-v_z^2/v^2)$, where $v=\sqrt{2T/M}$ gives the temperature T in energy units of particles of mass M. Here, we refer to T so defined as the particle temperature (or energy) noting that the velocity distribution function is probably not an exact Maxwellian. The quantity v will be called the particle velocity. The corrected profile for Fig. 5(a) (here, the main correction is due to the system spectral resolution) yields an energy of $\simeq 18$ eV, which corresponds to a velocity of 1.7 cm/μs, for the C III ions. The data indicated no line shift to within 0.01 Å (as will be shown in Sec. III C), thus the average velocity in the z direction for the C III ions is <0.13 cm/μs.

The edge effects due to the finite length l_z of the active anode were checked by repeating this measurement for $l_z=2$ and 14 cm (see Fig. 5) and found to be unimportant. This result was also obtained for the Mg II velocity distribution (see Sec. III B 6a). The independence of the line shape on the anode length l_z also showed that the effect of self-absorption is negligible, as will be further shown in Sec. III B 7.

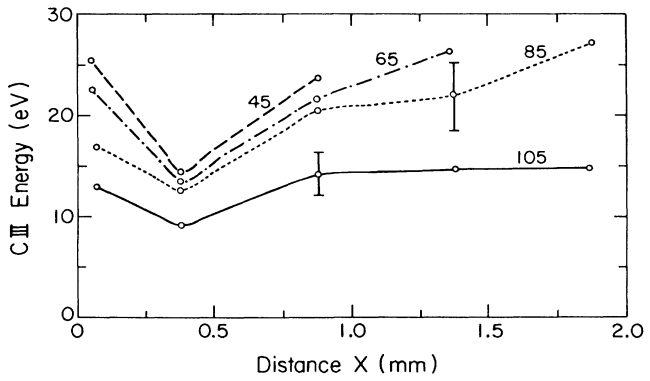

FIG. 6. C III energy obtained from the 2297-Å line as a function of distance from the anode surface for four times given in nanoseconds. The uncertainty in the energy is ±15% as indicated.

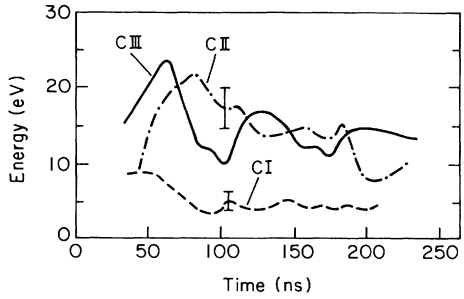

FIG. 7. Position-averaged energy for C III, C II, and C I obtained from the 2297-, 2512-, and 2479-Å lines, respectively. Here, $l_z=l_s=4$, 14, and 14 cm, respectively. The uncertainty is ±15% as indicated.

The C III energy as a function of time and distance was obtained with a short anode ($l_z=2$ cm) which made possible a spatial resolution $\lesssim 0.3$ mm. The axial distribution of the C III energy is shown in Fig. 6 for four times. During the pulse ($t\lesssim 95$ ns) the energy is seen to be between 15 and 25 eV. This relatively high energy is found in the entire plasma and it decreases in time. By moving the system line of sight behind the anode we could observe a region near the anode surface only $\simeq 100$-μm wide. From these measurements we concluded that the ions acquire their energy very close to the anode surface.

In Fig. 7 we plot the C III energy, averaged over the entie plasma, obtained with an anode of $l_z=4$ cm as a function of time. For this average the energy at each position is weighted by the line intensity at the same position. The energy is seen here to decrease for $t\gtrsim 60$ ns.

Figure 7 also shows the velocity distributions for neutral carbon atoms and singly charged carbon ions. For these measurements we used the 2479-Å line for C I and the 2512- and 3921-Å lines for C II. The C II energy, which rises to about 20 eV, is close to that of C III. The C I energy is about 7 eV, smaller than the C II and C III energies. After the pulse all energies are lower than during the pulse. The energy decrease in the second half of the pulse occurred for most of the species observed (see below). In some of the discharges the C II and the C III energy rose early in the pulse as shown in Fig. 7.

3. *Velocities of ions and neutral particles*

Carbon particles are believed to originate, to a large extent, from adsorbates of hydrocarbons on the anode surface, as discussed in Ref. 12. We, therefore, observed the energies of particles ejected from the dielectric material in order to examine whether these particles have energies similar to those of the carbon particles. We also observed the velocities of various singly charged ions in order to examine the energy dependence on the ion mass. In these experiments the epoxy anode was mixed with MgF_2, CaF_2, and $AlNaSiO_3$, each constituting 20% by

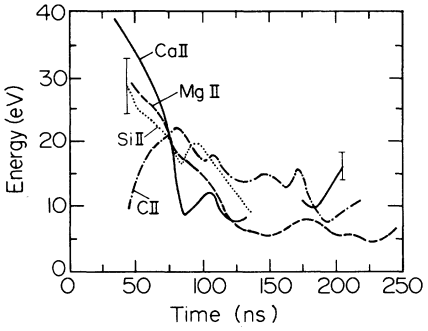

FIG. 8. Position-averaged energies of C II, Mg II, Si II, and Ca II using a 14-cm-long anode with an admixture of MgF_2, CaF_2, and $AlNaSiO_3$, each constituting 20% by weight of the entire mixture. The lines observed were at 2512, 2798, 4131, and 3179 Å, respectively. The uncertainty is ±15% as indicated.

weight of the entire mixture. The position-averaged C II, Mg II, Si II, and Ca II energies observed with this anode are presented in Fig. 8 (the C II data are taken from Fig. 7). The energies of Mg II, S II, and Ca II decrease from $\gtrsim 30$ eV at the beginning of the pulse to $\simeq 15$ eV at the end of the pulse. For $t < 80$ ns, the C II energy is seen to rise to $\simeq 20$ eV. To within the experimental uncertainty the energies of Mg II, Si II, and Ca II are the same.

In order to further examine possible dependence of the energy on the ion mass we attempted to measure the energy of much heavier ions. Thus, we observed the spectral profile of the Ba II 2634-Å line using an epoxy admixture that contained 60% by weight BaF_2. However, the Doppler broadening for the Ba II ions was too small to be measured. The observed spectral profile of the 2634-Å line is given in Ref. 16. This profile, corrected for the system spectral resolution and the Zeeman splitting gave an upper limit of 30 eV for the Ba II ions. These results show that all singly charged ions observed have similar energies.

Velocities of neutral particles other than C I were also observed. The B I energy was observed using the 2498-Å line (with the epoxy anode mixed with 43% by weight of B_2O_3 powder and $l_z = 12$ cm) and the Mg I energy using the 2852-Å line (38% by weight of MgF_2 and $l_z = 9$ cm). The B I and Mg I energies were found to be $\simeq 5$ and 9 eV, respectively, similar to the C I energy.

4. *The energies of doubly and triply charged ions*

We attempted to compare the C III energy to energies of other doubly and triply charged ions. The B III velocity was observed using an anode with the epoxy mixed with B_2O_3 (43% by weight). The active anode length l_z was 14 cm and the boron region was 2-cm long ($l_s = 2$ cm) in order to avoid optical thickness effects. Using the 2066-Å line the B III energy was found to vary during the pulse between 15 and 28 eV, similar to the C II and C III energies. The Si III and Si IV velocities were observed using two different anode admixtures as given in Fig. 9. The Si III energy for one admixture, obtained using the

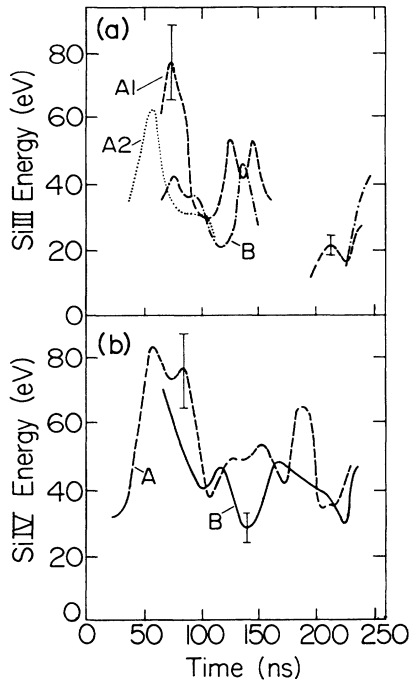

FIG. 9. (a) Si III energy, obtained using the 2559- and the 3242-Å lines (shown by the curves *A* 1 and *A* 2, respectively), for an epoxy mixture containing 50% by weight $AlNaSiO_3$. Also shown is the energy obtained from the 2559-Å line using a mixture containing MgF_2, CaF_2, and $AlNaSiO_3$, each 20% by weight (curve *B*). (b) Si IV energy, obtained using the 3166-Å line, for the $AlNaSiO_3$ anode (curve *A*) and the MgF_2, CaF_2, and $AlNaSiO_3$ anode (curve *B*). The uncertainties are ±15% as indicated.

2559-Å and 3242-Å lines, are shown by the curves *A* 1 and *A* 2 in Fig. 9(a). The Si III energy obtained with the other admixture, using the 2559-Å line, is shown by the curve *B* in Fig. 9(a). The Si IV energy, obtained using the 3166-Å line, is shown for the two anodes by the curves *A* and *B* in Fig. 9(b). The Si III energy is between 30 to 80 eV and the Si IV energy appears to be similar to the Si III energy. This is larger than the energy of Si II (Fig. 8) and than the energies of the other multiply-charged ions (C III, see Fig. 7, and B III), which are similar to the C II energy. The C IV energy could not be measured because the line emission was too weak.

5. *Dependence of the particle energies on the dielectric mixture*

The particle energies appear to be insensitive to the epoxy admixture used for the anode. The Mg II energy was also observed using an anode mixed with 38% by weight of MgF_2 powder, giving a similar result to that shown in Fig. 8 obtained with a different admixture. Another example for the insensitivity to the admixture can be seen in the Si IV energies shown in Fig. 9(b), where the general behavior of the Si IV energy is similar for the two anodes (curves *A* and *B*).

6. *Dependence of the particle energies on experimental parameters*

(a) *Location over the anode.* The diode geometry is asymmetric in the y direction: electrons are emitted from the protruding cathode vane at the top of the diode and stream downward by $\mathbf{E}\times\mathbf{B}$ drift. We examined whether the ion lateral velocities in the anode plasma vary along this direction. To this end we measured the C III velocity distribution, using the 2297-Å line, in different discharges in which the diagnostic system collected light only from the top one-third or from the bottom one-third of the anode. No difference between the observed C III velocities was seen for the these two cases.

The dependence of the velocities on z was tested by measuring the Mg II velocity distributions (using the 2937-Å line) in experiments in which the MgF_2 powder was mixed with the epoxy in 2-cm-long regions ($l_s=2$ cm), located at $z=+5$ and -5 cm relative to the anode center. In these experiments the active anodes were 14-cm long ($l_z=14$ cm). The velocity distributions measured here were the same as those found with a 14-cm-long anode seeded with MgF_2 along its full length.

The intensities of Mg II lines emitted from the two anode regions at $z=\pm5$ cm were very similar. Also, ion current densities measured between $z=-4$ and $+4$ cm using charge collectors were uniform within $\pm15\%$. This shows that the anode plasma was fairly uniform along the z direction.

(b) *Dielectric structure and material.* Visual examination of the surface of a newly made active anode showed about up to 20-μm-deep grooves caused by machining. We checked whether such roughness of the surface had an effect on the observed velocities. For these experiments we used an anode of $l_z=2$ cm with the anode surface polished to better than 1 μm. The C III energy observed using the 2297-Å line was similar to that obtained with the regular anode.

The C III velocity was also observed for an active anode made of a polyethylene sheet (rather than epoxy). The macroscopic nonuniformity in the polyethylene sheet (believed to induce faster surface flashover) was formed by drilling 0.8-mm-diam holes 3-mm apart. The C III energy was also measured for a 2-cm-long epoxy anode with no metal structure in the active anode. The results were similar to those of the standard experiments.

Finally, we measured the C III velocity distribution for an anode in which the grooves were perpendicular to the magnetic-field lines (and to the line of sight). The energies obtained were somewhat smaller, 8–13 eV.

(c) *Applied magnetic field.* The dependence of the ion energy on the applied magnetic field B_z was examined by observing the C III energy using the 2297-Å line in similar experiments with $B=5.5$, 7.2, and 9.0 kG. The position-averaged C III energies for these values of B_z are shown in Fig. 10 for five times. It is seen that during the main pulse ($t<95$ ns) the C III energy is larger for stronger magnetic fields. After the pulse the dependence is weaker.

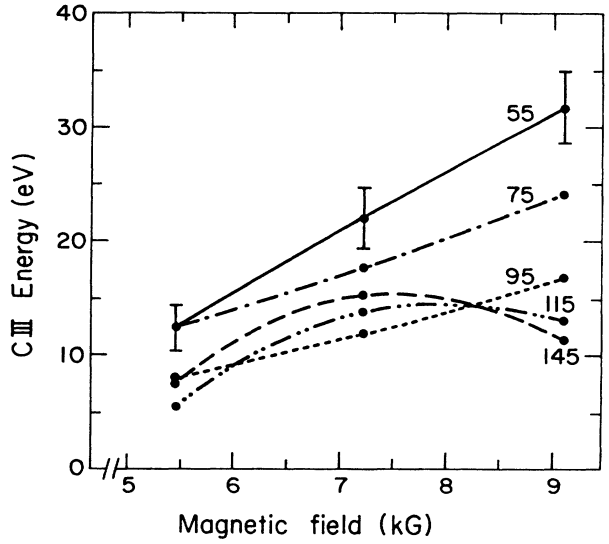

FIG. 10. Position averaged C III energies observed using the 2297-Å line for three different applied magnetic fields, for five times indicated in nanoseconds. Here, $l_z=4$ cm. Each data point represents three measurements and the uncertainty is $\pm10\%$ as indicated. The smooth lines connect the data points.

7. *Examinations of the plasma optical depth*

We utilized experiments with various anodes to examine the plasma optical thickness by two kinds of observations. In the first kind we repeated line-spectral-profile measurements for various lengths l_s [see Fig. 1(c)] of the line-emitting region of the plasma. An increase in the line intensity with l_s together with a spectral line profile unaffected by l_s indicates the absence of self-absorption effects. In these experiments we observed self-absorption effects only for our strongest observed line, the C III 2297-Å line. An increase of the linewidth by $\lesssim10\%$ was seen when the anode length was changed from $l_z=l_s=2$ cm to $l_z=l_s=14$ cm. Our energy measurements for C III are based on spectral profiles measured with anode lengths ≤4 cm, thus ensuring the absence of optical thickness effects. The self-absorption of our other strong lines, the Mg II 2937-Å, 2798-Å, and 2796-Å lines, were examined by measuring the spectral profiles of these lines in identical experiments. The first two lines ($4s\rightarrow3p$ and $3d\rightarrow3p$, respectively) are absorbed by the same $3p$ level with the absorption cross section for the 2798-Å line being about six times larger than for the 2937-Å line. Thus, optical thickness effects would be six times stronger for the 2798 Å. The third line (the 2796-Å, $3p\rightarrow3s$ line) is expected to be thicker than the previous two lines since it is absorbed by the ground state. The spectral widths of the three lines, observed with our longest active anode ($l_s=14$ cm), gave the same Mg II velocity distribution to within the experimental error. This demonstrates the absence of optical thickness effects for these lines. Such examinations have also been made for the 3934- and the 3968-Å lines of the Ca II multiplet $4p\rightarrow4s$ (that differ in self-absorption by a factor of 2) giving the same result.

Besides testing the optical thickness effects, the observation of particle velocities using different lines of the same species verified the absence of interference by impurity lines and provided additional checks of our error estimates.

C. Velocity distribution perpendicular to the anode

The purpose of the measurements described in this section was to observe the particle-velocity distribution perpendicular to the anode including the determination of the average velocity in this direction. For these measurements the optical system must look normal to the surface, thus light is collected from a small region of the plasma. Therefore, only our strongest line, the C III 2297-Å line, could provide a sufficiently large light signal. For this measurement we aligned our system to look at 53° with the normal to the surface, as shown in Fig. 11. The light path in the plasma was then about 2.5 mm. With this direction of sight the velocity components in the z direction also contribute to the spectral line profile, which was accounted for in the data analysis. A 7-mm-wide slot in the y direction was cut in the cathode to allow the light from the central region of the anode to reach the spectroscopic system. Light from the cathode plasma in the cathode-slot region was checked to appear too late to interfere with the measurement for times up to 200 ns.

In this measurement light is collected from the entire axial extent of the plasma. Since the line intensity varies with the distance x (see Fig. 4) the measurement gives mainly the particle velocity in the region of strong line emission. Thus, observing the Doppler-broadened profile of the C III 2297-Å line for $t=75$ ns, for example, gives mainly the C III ion-velocity distribution in the region $x=0.2$ to 1.2 mm (see Fig. 4).

To obtain the average velocity perpendicular to the anode the absolute line shift must be determined. We centered the spectrograph on the C III 2297-Å line using the close 2302-Å line of a mercury lamp. However, because of the spectrograph drift and the small line shift we performed 13 identical measurements in order to obtain the line shift with satisfactory accuracy. The line was found to be blue shifted with the shift as a function of time shown by the curve N in Fig. 12. The indicated error bars were determined by the standard deviation (0.045 Å) divided by $\sqrt{12}$. In order to further substantiate the accuracy in the observed shift we performed 12 identical measurements, using the same procedure, but looking in the z direction (as in Sec. III B 2). The observed line shift is given by the curve P in Fig. 12, showing zero average velocity in the z direction (as stated in Sec. III B 2).

The linewidth observed in the 53° direction was similar to the width in the parallel-to-anode observation. We estimate that a difference of less than a factor of 2 between the widths of the parallel and the perpendicular velocity distributions could not be noticed using the line of sight of 53°. The similarity of the two observed widths is, therefore, consistent with a perpendicular velocity distribution equal to the positive half (i.e., away from the anode surface) of a Gaussian distribution that is similar to the parallel distribution. The average positive velocity perpendicular to the anode would then be $U=0.57\sqrt{2T(\text{C III})/M(\text{C})}$, where $M(\text{C})$ and $T(\text{C III})$ are the carbon mass and the C III temperature observed in parallel observation, respectively. We used the time-dependent $T(\text{C III})$ averaged over position weighted by the line intensity. The calculated line shift for the line of sight at 53° with the normal, corresponding to the average velocity thus obtained, as shown by the curve A in Fig. 12. This calculated line shift decreases in time since the velocities parallel to the anode decrease in time. In

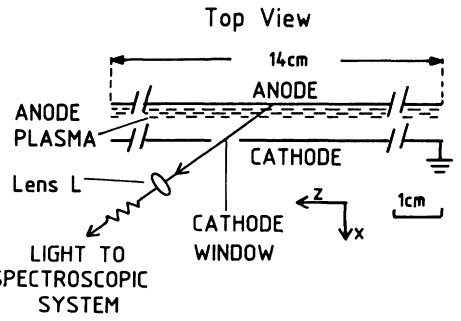

FIG. 11. Schematic of the arrangment used for measuring the line-emission spectral profile at an angle $\theta=53°$ with the normal to the anode. The line of sight was in the x-z plane, inclined in the $+z$ direction. The system viewed the central part (of length $\Delta z=6$ mm) of the 14-cm-long active anode. A slot, 4 cm high and 0.7 cm wide (in the z direction), was cut in the cathode to allow the passage of light to the spectrometer. The other slots in the cathode, used for the ion transmission, were as before (see Fig. 1).

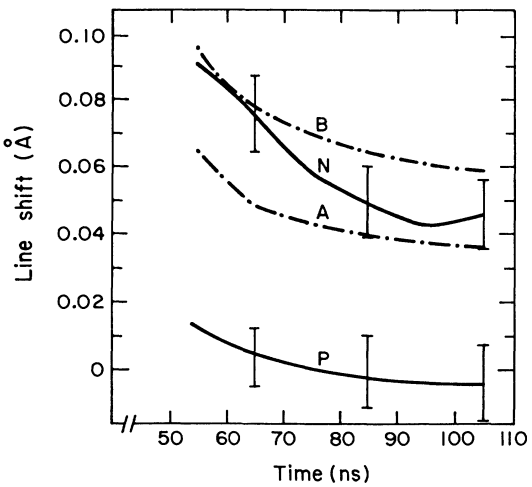

FIG. 12. The blue shift of the C III 2297-Å line measured at 53° with the normal to the anode (N) and the shift measured parallel to the anode (P). Each point on the N and P curves is an average of 13 and 12 discharges, respectively. The line shift which corresponds to the average of the positive half of the time dependent C III velocity distribution, observed parallel to the anode, is given by curve A. Curve B corresponds to twice this average velocity (see text).

Fig. 12, we also plot by the curve B the line shift that corresponds to an average axial (positive) velocity equal to $2U$. The comparison of the measured line shift with the curves A and B indicates that the average C III velocity is within a factor of 2 of the average of the positive half of the parallel velocity distribution. From this and from the observed linewidths it appears that the C III velocity distribution perpendicular to the anode is close to the positive half of a Gaussian distribution that corresponds to the observed temperature T(C III). This result is used in Ref. 12 to describe the particle flow and density profiles in the plasma.

D. Electron-density distribution

The electron density was measured as a function of time and distance from the anode surface by observing the Stark broadening of the hydrogen H_β line as was done by Pal and Hammer.[8] However, in this measurement the line Doppler broadening must be taken into account. We attempted to obtain the hydrogen velocity from the Doppler broadening of the H_α line. However, the uncertainties in the calculations[21,25,26] of the Stark broadening of this line for the present electron density and ion temperature did not allow us to obtain the Doppler broadening reliably. Since the velocity distributions for all the neutral particles observed in our plasma (C I, B I, Mg I) showed a temperature of 5–10 eV, it was reasonable to assume a temperature of 8 eV for the neutral hydrogen particles. This was supported by the fact that at $x \geq 0.75$ mm the FWHM of the H_α line was observed to be about 2 Å. In order to deconvolve the Doppler contribution to this observed width of the H_α line we assumed a Stark broadening as measured by Ehrich and Kelleher[26] for 2-eV proton perturbers. While the proton temperature in our plasma is probably higher than 2 eV (as all temperatures observed for other singly charged ions are, see Sec. III B), the H_α Stark broadening appears to be insensitive to the proton temperature in this parameter range.[26] The Doppler broadening obtained from this deconvolution gives a hydrogen temperature of $\simeq 9$ eV.

The electron density was, therefore, unfolded from the H_β linewidth assuming a Doppler broadening with a FWHM of 1.05 Å for this line, corresponding to a hydrogen temperature of 8 eV. The uncertainty in the Doppler broadening dominated the error (±20%) in determining the electron density.

The electron density as a function of the distance x from the anode surface was measured for short ($l_z = 2$ cm) and long ($l_z = 8$ cm) active anodes, giving the same results. The axial variation of the electron density $n_e(x,t)$ for the short anode is given for five times in Fig. 13. The spatial resolution in these measurements was about 0.3 mm. The earliest time at which the plasma density is measured is 25 ns. The plasma then expands with its density increasing. The plasma density could not be measured far from the anode surface (at $x > 1.5$ mm) until $t = 75$ ns because of the low H_β intensity there. Quantitative analysis of the rise of the electron areal density in the plasma is given in Ref. 12.

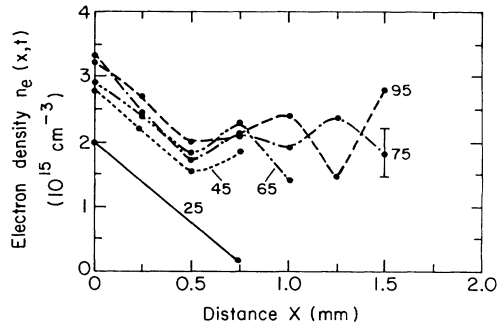

FIG. 13. Measured electron density $n_e(x,t)$ as a function of the distance x from the anode surface for five times given in nanoseconds. The data points are connected by smooth lines. The active anode length is $l_z = 2$ cm and the spatial resolution is $\lesssim 0.3$ mm. The error is ±20% (as indicated), resulting mainly from the uncertainty in the H_β Doppler broadening.

IV. DISCUSSION

A. Early fast plasma expansion

In our experiments line emission was first observed at $t \simeq 20$ ns, and at $t \simeq 55$ ns the plasma was seen to occupy an approximately 1.5-mm-wide region near the anode surface, giving an expansion velocity of at least 3 cm/μs. This early expansion of the plasma was found to be insensitive to the applied magnetic field of 5–9 kG. The applied field was observed to be present in the plasma from a few nanoseconds after its appearance, i.e., at $t \simeq 25$ ns, and throughout the entire pulse.[16] We have not as yet experimentally investigated the plasma expansion early in the pulse because of the absence of spontaneous light emission during this period.

It was initially suggested[27] that the high plasma expansion velocity could be explained by high ion velocities accompanied by low-temperature electrons. The high collisionality of the low-temperature electrons would make fast expansion of the plasma in the magnetic field possible. However, Litwin and Maron[28] showed that electrons would be rapidly heated during the expansion due to elastic collisions with the hotter ions, thus causing the plasma to slow down before it expanded.

The insensitivity of the early fast plasma expansion to the applied magnetic field and the presence of the magnetic field in the plasma at the time of its appearance led to a suggestion of an alternative mechanism of the plasma expansion after a similar suggestion by Prono *et al.*[29] This mechanism is based on the formation of a fast-neutral-particle layer by charge-exchange processes and the subsequent ionization of the layer. The calculated expansion and ionization of the neutral particle layer[28] were in a reasonable agreement with the plasma thickness and density observed a few nanoseconds after the plasma appeared, given in Sec. III.

B. Plasma particle velocities

Neutral particles and ions in the plasma originating from contaminants on the dielectric anode surface and

from the dielectric material proper have been observed in the present study to have energies parallel to B_z of about 5 to 10 eV for the neutral particles and 20 to 80 eV for the ions. These energies are observed throughout the entire voltage pulse and over the entire plasma to within a distance of $\simeq 100$ μm from the anode surface. The energy of the C III ions was found to be insensitive to the metal structure or to the dielectric material and surface roughness. The C III energy increased somewhat with the applied magnetic field.

The C III ions were found to move away from the anode surface with a velocity distribution which was close to the positive half of the Gaussian-like distribution parallel to the anode. In Ref. 12 we show that during and after the voltage pulse the observed particles are continuously injected from the anode surface into the plasma.

The mechanisms of particle release from the dielectric surface during and after its electrical breakdown are not well understood. Particles can be released from the surface due to bombardment by plasma particles. Impact of plasma electrons of a few electron volts may desorb neutral particles from the surface with a yield of about unity.[30] However, energies of neutral particles released by this process are believed to be 1 eV or less,[31–34] significantly smaller than observed here. Positive ions may desorb with kinetic energies of several electron volts,[35,36,33] again smaller than the presently observed ionic energies. It is possible that electrical charging of the dielectric anode surface by electrons accelerated in the diode is responsible for the ejection of particles from the anode dielectric material as well as for the observed particle velocities. However, no information on such processes for the parameter range of our diode voltage and current is available. Another possible mechanism by which ions produced at the anode surface may be accelerated into the plasma is negative charging of the anode plasma with respect to the anode surface. In the presence of magnetic fields, ion flow across these fields may be more rapid than electron flow. Hence, the plasma would be expected to charge negatively relative to such surfaces.[37] We also note that the production of fast ions on the surface can lead to the fast neutral particles observed via charge-exchange processes there. These issues require further investigation.

The fact that the neutral-particle and the singly charged ion energies in the plasma significantly differ from each other ($\simeq 7$ and $\simeq 18$ eV for C I and C II; $\simeq 9$ and $\simeq 25$ eV for Mg I and Mg II) suggests that a large fraction of the singly charged ions are not produced by neutral ionization in the plasma, but rather have an independent origin, apparently in the immediate vicinity of the anode surface, where the particles presumably acquire their kinetic energies. This conjecture was supported by spectroscopic observations[12] that quantitatively determined the time-dependent particle fluxes from the surface into the anode plasma for various charge states. During the voltage pulse the fluxes of neutral particles from the anode surface into the anode plasma are much smaller (to a different extent for different elements) than those of the singly charged ions. The ionization of neutral particles can thus account only for a small fraction of the singly charged ions in the plasma. The remainder of these ions was shown in Ref. 12 to come directly from the vicinity of the anode surface.

The doubly charged carbon ion energy was found to be similar to that of the C II ions ($\simeq 20$ eV). However, Si III and Si IV ions were found to be more energetic (40–80 eV) than Si II (20–30 eV) and than C III and B III ($\simeq 20$ eV). A plausible explanation for the relatively large energy of the Si III and the Si IV ions is also discussed in Ref. 12.

The particle-velocity distributions parallel to the anode were found to be nearly isotropic. The reason for this is probably rapid collisional thermalization near the anode surface. For example, for thermalization to occur for C III ions, assuming mainly collisions with protons, a proton density of $\simeq 10^{18}$ cm^{-3} over 10 μm is required. This is possible considering the high particle densities believed to exist near surfaces undergoing electrical breakdown.[38] The use of the positive half of a Gaussian distribution to describe the axial velocities of the ions in the plasma is consistent with this model, in which the ions thermalize in the very immediate vicinity of the anode surface before they move away from the surface.

Knowledge of the ion energies yields the ion Larmor radii in the plasma. For the nonprotonic ions the Larmor radii under the $\gtrsim 7$ kG magnetic field are comparable or larger than the plasma thickness. The proton energy could not be measured. However, since the energies of all the singly charged ions observed (C II, Mg II, Si II, and Ca II) were between 15 to 35 eV (see Fig. 8), we assume a similar energy for the protons. For 25-eV protons, the Larmor radius is $\simeq 0.7$ mm, i.e., about $\frac{1}{3}$ of the plasma thickness. The implications of the relatively large Larmor radii of the nonprotonic ions on the ion flow in the plasma and the ion extraction are interesting issues that need further study.

It is interesting to compare our measured ion-velocity distribution in the anode plasma parallel to the anode and to the magnetic-field lines to that measured in the same direction in the diode acceleration gap (the region between the anode plasma and the cathode plasma). The latter measurements were previously made[20] in a similar diode configuration. The present results show that the ion velocities in the plasma parallel to the electrodes can account for about $\frac{1}{3}$ of the velocities in the gap. The ion velocities in the plasma determine a lower limit for the divergence of the generated ion beam. For our anode (270 kV) this lower limit of the mean angular divergence is about 0.4°. If the ion velocities in the plasma parallel to the anode would not increase for higher-voltage diodes the divergence angle would be sufficiently small to allow beam application in inertial confinement fusion.[3] However, the ion velocities for other plasma sources, currently under development for this application,[39] will have to be examined.

C. Electron heating

Using measured line-emission intensities and time-dependent collisional-radiative calculations, we have determined[13] the electron temperature in our anode plas-

ma to be $T_e \simeq 7$ eV,[15] i.e., lower than the ion temperature T_i. Electron elastic collisions with ions, therefore, would not cool the electrons, as was commonly believed, rather they will contribute to the electron heating. The average rate of energy gained by an electron in such collisions is

$$Q = 3\frac{m_e}{m_i}\nu_{ei}(T_i - T_e) , \quad (1)$$

where m_e and m_i are the electron and ion masses, respectively, and $\nu_{ei} = 2.6\times10^{-6} n_i z^2 \ln\lambda / T_e^{3/2}$ s^{-1} is the electron-ion Coulomb collision frequency.[16] Here, z, n_i, and $\ln\lambda$ are the ion charge, the ion density, and the Coulomb logarithm, respectively. Assuming, for simplicity, a plasma composed of 25-eV protons and 7-eV electrons with an average density 2.2×10^{15} cm^{-3} (see Fig. 13), one obtains an electron heating rate $\frac{2}{3}Q \simeq 0.06$ eV/ns. This electron heating rate is about $\frac{1}{3}$ of the Ohmic heating rate due to the currents in the plasma that is estimated in Ref. 15.

D. Plasma expansion against the magnetic field

The observed relatively high ion temperature in the plasma is expected to enhance the plasma expansion against the magnetic field. We now use the observed ion temperature, the electron density, the electron temperature,[15] and the fact that the applied magnetic field in the diode penetrates the plasma[16] to calculate the expected plasma expansion velocity after the initial plasma formation (i.e., at $t \gtrsim 20$ ns). For this estimate we assume that the plasma is fully ionized since electron and ion collisions with the neutral hydrogen particles of a concentration of $\simeq 30\%$ (Ref. 12) have negligible effect on the expansion. We assume a proton-electron plasma and we use a one-dimensional fluid treatment. The use of a fluid treatment is reasonably justified since the proton Larmor radius $r_p \simeq 0.7$ mm is smaller than the plasma thickness ($\simeq 1.5$–2 mm), and the inverse proton-cyclotron frequency is 14 ns, shorter than the pulse length ($\simeq 80$ ns). Thus we use the formula for the expansion velocity[40]

$$v_{ex} = -\frac{c^2}{\sigma B^2}\partial_x P , \quad (2)$$

where σ is the electric conductivity, P is the plasma pressure, and $\partial_x P = \partial P/\partial x$. In using this formula we neglected the convective terms, which is justified since the expansion velocity is significantly smaller than the ion sound velocity.

We now assume that $P = n(T_i + T_e)$ with $T_i = 25$ eV and $T_e = 7$ eV, a plasma density $n = 2.2\times10^{15}$ cm^{-3}, a pressure-gradient scale of 1 mm, and $B = 7.6$ kG as observed[16] in the plasma. Assuming classical electron conductivity[17] (i.e., electron collision frequency ν_{ei}) gives $v_{ex} \lesssim 0.1$ cm/μs, which is much smaller than the observed velocity ($\simeq 1$ cm/μs, see Sec. III A). This result is not affected by the presence of non protonic ions in the plasma since these ions are estimated to have little effect on the plasma conductivity.

The plasma motion is significantly affected by the currents in the Y direction induced in the plasma by the electron flow in the diode acceleration gap. Using a classical conductivity we estimate these currents from the time dependent component of the magnetic field on the anode side obtained from the observation of Zeeman splitting.[16] The $\mathbf{J}_y \times \mathbf{B}$ forces are estimated from the induced current density J and the observed magnetic field in the plasma. These forces are expected to push the plasma back to the anode surface with a velocity > 1 cm/μs, in contradiction to the observations.

We now show that the anode plasma in our experiment may be unstable to the lower hybrid-drift instability in the low-drift velocity regime.[18,19] We then show that the resulting anomalous plasma conductivity may allow the plasma to expand at the rate observed. The electron drift velocity v_d can be obtained from the current density j_y in the plasma which is derived from the plasma pressure gradient. Using the momentum equation $j_y B/c = \partial_x P$ (the convective terms are small) a current density $j_y \simeq -1600$ A/cm^2 is obtained. The resulting electron drift velocity, assuming no ion drift in the y direction, is then

$$v_d = -\frac{j_y}{en} = -\frac{c}{eB}(T_i + T_e)\frac{\partial_x n}{n} , \quad (3)$$

giving $v_d \simeq 0.7 v_{th}$, where v_{th} is the thermal velocity of 25-eV protons. This may make the plasma unstable to the lower hybrid-drift instability in the low-drift velocity regime.[18,19]

The case of the low-drift velocity for $T_e < T_i$ was analyzed by Davidson and Gladd[18] and by Davidson.[19] An estimate of the growth rate γ is obtained from

$$\gamma = \frac{\sqrt{2\pi}}{8}(\omega_{ce}\omega_{ci})^{1/2}(v_d/v_{th})^2 , \quad (4)$$

where ω_{ce} and ω_{ci} are the electron and the ion cyclotron frequencies, respectively. This gives γ^{-1} of about 2 ns, much shorter than the pulse length. The k vector in the direction perpendicular to $\mathbf{B}$, $k_y = \sqrt{2T_e/T_i}/r_e$ (where r_e is the electron Larmor radius),[18] is about 100 mm^{-1}. Thus, $1/k_y$ is smaller than the plasma thickness as required and the instability can grow.

The anomalous collision frequency ν_a has been discussed in Refs. 18 and 19. We use the formula given by Davidson,[19] corroborated by simulation calculations.[41] For $\omega_{pe}/\omega_{ce} > 1$ (in our case $\omega_{pe}/\omega_{ce} \simeq 20$), ν_a is given by

$$\nu_a = \frac{\sqrt{2}}{45}\omega_{ce}^2(\omega_{ce}\omega_{ci})^{-1/2}(v_d/v_{th})^5$$
$$\approx 2\times10^{11}(v_d/v_{th})^5 \text{ s}^{-1} . \quad (5)$$

We use the anomalous frequency ν_a which corresponds to the instability stabilization by ion trapping with disregard to stabilization due to the relaxation of the current density j_y, as discussed by Chen and Birdsall.[41] This is because the pressure in our plasma is maintained throughout the pulse, thus causing the current density j_y (and the electron drift velocity) to remain high.

We then assume that the anomalous electron conductivity can be estimated by (see discussions in Refs. 42 and 43)

$$\sigma_a = ne^2/m_e\nu_a \ . \tag{6}$$

Equations (5) and (6) give $\sigma_a \simeq 2\times 10^{13}\ \mathrm{s}^{-1}$, i.e., an anomalous conductivity about ten times lower than the classical conductivity. It is shown in Ref. 15 that such a conductivity reduces the current density induced in the plasma by the electron flow in the diode gap to a value that is much lower than the pressure-driven current density $j_y = c\partial_x P/B$. This is consistent with the use of j_y in Eq. (3) to estimate the electron drift velocity and it also means that the induced current density would not affect the plasma motion significantly. Thus, Eq. (2) can now be used with $\sigma = \sigma_a$ to obtain an estimate for the anomalous plasma expansion velocity v_{exa} giving 1 cm/μs, which is in agreement with the observations. We emphasize, however, the sensitivity of the anomalous collision frequency to the electron drift velocity v_d. Also, the theoretical treatment[18,19] we used assumed a collisionless plasma.

The growth rate of the instability [Eq. (4)] and the anomalous collision frequency [Eq. (5)] increase with the ion temperature since higher ion temperature proportionally increases the plasma pressure and the resultant current density j_y. The relatively short growth time and high collision frequency in our plasma are, hence, largely due to the relatively high ion temperature. The current density j_y also dominates the plasma heating as discussed in Ref. 15. The current in the plasma due to the ion extraction into the diode gap has been neglected in the present discussion since the ion current density of $\lesssim 100$ A/cm^2 is much smaller than j_y. We note that the effect of the instability on the ion temperature is small since the Ohmic heating per particle due to the pressure-driven currents in the plasma is estimated to be smaller than the ion temperature.[15].

The plasma flux nv_{ex} perpendicular to the anode using $n = 2.2\times 10^{15}$ cm^{-3} and $v_{ex} = 1$ cm/μs is about three times larger than the extracted ion current density which peaks at about 100 A/cm^2. Thus, erosion of the plasma due to the current extraction does not limit the plasma expansion into the diode gap.[44] An additional source of plasma flux, although smaller than the total ion current density, is the ionization of neutral hydrogen atoms in the plasma. It is shown in Ref. 12 that hydrogen is continuously ejected from the anode surface into the anode plasma throughout the pulse. Assuming an energy of 8 eV for the hydrogen atoms (see Sec. III D), the ionization of these atoms as they traverse the plasma is calculated using the observed electron temperature, the measured electron density, and the observed absolute hydrogen ejection rate from the surface into the plasma.[12] The resulting hydrogen ionization in the outer region of the plasma produces a proton flux that is similar to the density of the proton current extracted from the plasma.

While in the present publication we used the observed plasma pressure to explain the plasma expansion rate, the continuous material ejection from the surface into the plasma and the ionization processes that determine the time-dependent plasma density are discussed in detail in Ref. 12. In brief, the plasma inventory increases throughout the pulse mainly due to the ionization in the plasma of hydrogen and C I, and due to continuous supply of protons and carbon ions from the immediate vicinity of the anode surface.

V. SUMMARY

Line Doppler-broadening and Doppler-shift measurements in the surface-flashover-produced anode plasma in a magnetically insulated gap showed that the velocity distributions of neutral particles and ions parallel to the anode surface are nearly Gaussian corresponding to mean kinetic energies about 8 eV for neutral particles, about 20 eV for singly charged ions, and 20–80 eV for doubly and triply charged ions. The ions were found to acquire their velocities very close to the anode surface and to move away from the anode surface with a nearly isotropic (in half of the velocity space) velocity distribution. A plausible explanation for the different energies for different charge states and for different elements of the same charge state, based on the presence of electric fields at the immediate vicinity of the anode surface, is discussed in Ref. 12.

The observed ion velocities in the plasma parallel to the anode are about $\frac{1}{3}$ of the velocities in the same direction previously observed in the diode acceleration gap.[20] The velocities in the plasma set a lower limit to the angular divergence of ion beams extracted from the diode.

The mean ion kinetic energy is larger than the observed electron temperature. This causes electron heating due to the ion-electron elastic collisions. The relatively high ion temperature also causes a large plasma pressure gradient (obtained using the observed electron density) which enhances the plasma expansion against the magnetic field. We suggest that the plasma conductivity is $\simeq 10\times$ lower than the classical conductivity. This conductivity causes a reduction in the currents induced in the plasma by the time-dependent electron flow in the diode acceleration gap (that tend to inhibit the plasma expansion) and also enhances the plasma expansion due to the plasma-pressure gradient. The observed plasma-pressure gradient and the suggested anomalous conductivity thus explain the fast plasma expansion against the magnetic field. It is shown that the anomalous plasma conductivity may be associated with the lower hybrid-drift instability in the low-drift velocity regime,[18,19] driven by the electron drift resulting from the relatively high plasma-pressure gradient. The anomalous plasma conductivity is shown[16] to be consistent with the penetration into the plasma of the time-dependent component of the magnetic field in the diode and with the observed uniformity of the electron temperature in the plasma.[15] The current due to the plasma-pressure gradient, together with the anomalous conductivity, is shown to be responsible for the electron heating during the pulse.[15]

In higher power diodes the higher plasma-pressure gradient may result in a fast plasma expansion. A limiting expansion velocity would then be the ion thermal velocity, which is about 5 cm/μs for 25-eV protons. This may explain the expansion velocity of 5–10 cm/μs inferred by Johnson and co-workers[7] from the diode-impedance behavior for their surface-flashover plasma.

The result that the singly charged ions in the plasma have higher energies than the neutral particles lends support to the observation[12] that ions mainly flow from the immediate vicinity of the anode surface into the plasma rather than being produced by ionization of neutral particles in the plasma. This demonstrates that observations of particle-velocity distributions in plasmas formed over surfaces can be used in studying material ejection from the surface. The particle-velocity distributions observed here are used in Ref. 12 to describe quantitatively the particle motion and ionization in the plasma as a function of time and distance from the anode surface and thus to predict the extracted fluxes of the various ions.

The processes responsible for the ion and neutral-particle kinetic energies and their spatial and temporal variations are not known as yet. They may be further studied in experiments with different dielectric structures and electric or magnetic fields. Investigations with plasma sources other than surface-flashover plasmas would be helpful to differentiate between various processes. We believe that studying the particle kinetic energies in pulsed plasmas would be helpful in the understanding of the plasma behavior and in the development of plasma sources for many applications.

ACKNOWLEDGMENTS

The authors are thankful to Z. Zinamon, A. E. Blaugrund, and H. R. Griem for critical discussions and careful reading of the manuscript. Thanks are due to E. Nahshoni and M. Markovits for help in the experiments. Valuable suggestions by G. Hazak, C. Litwin, A. Fisher, A. Fruchtman, M. E. Foord, and M. Strauss are gratefully acknowledged. The skilled technical assistance by P. Meiri and Y. Danino is appreciated.

[1]P. Dreike, C. Eichenberger, S. Humphries, and R. N. Sudan, J. Appl. Phys. **47**, 85 (1976).
[2]S. Humphries, Jr., Nucl. Fusion **20**, 1549 (1980).
[3]J. P. VanDevender, Plasma Phys. Controlled Fusion **28**, 841 (1986).
[4]D. J. Johnson, E. J. T. Burns, J. P. Quintenz, K. W. Bieg, A. V. Farnsworth, Jr., L. P. Mix, and M. A. Palmer, J. Appl. Phys. **52**, 168 (1981).
[5]R. N. Sudan and R. V. Lovelace, Phys. Rev. Lett. **31**, 1174 (1973).
[6]J. E. Maenchen, F. C. Young, R. Stringfield, S. J. Stephanakis, D. Mosher, Shyke A. Goldstein, R. D. Genuario, and G. Cooperstein, J. Appl. Phys. **54**, 89 (1983).
[7]D. J. Johnson, G. W. Kuswa, A. V. Farnsworth, Jr., J. P. Quintenz, R. J. Leeper, E. J. T. Burns, and S. Humphries, Jr., Phys. Rev. Lett. **42**, 610 (1979); D. J. Johnson, P. L. Dreike, S. A. Slutz, R. J. Leeper, E. J. T. Burns, J. R. Freeman, T. A. Mehlhorn, and J. P. Quintenz, J. Appl. Phys. **54**, 2230 (1983).
[8]R. Pal and D. A. Hammer, Phys. Rev. Lett. **50**, 732 (1983).
[9]J. Maenchen, L. Wiley, S. Humphries, Jr., E. Peleg, R. N. Sudan, and D. A. Hammer, Phys Fluids **22**, 555 (1979).
[10]Y. Maron, M. D. Coleman, D. A. Hammer, and H. S. Peng, Phys. Rev. A **36**, 2818 (1987).
[11]D. Hinshelwood, Naval Research Laboratory Memo, Report No. 5492, 1985 (unpublished).
[12]Y. Maron, L. Perelmutter, E. Sarid, M. E. Foord, and M. Sarfaty (unpublished).
[13]M. A. Sweeney, J. E. Brandenburg, R. A. Gerber, D. J. Johnson, J. M. Hoffman, P. A. Miller, J. P. Quintenz, S. A. Slutz, and K. W. Bieg, in *Proceedings of the Fifth International Conference on High Power Particle Beams, San Francisco, CA,* edited by R. J. Briggs and A. J. Toepfer (Lawrence Livermore National Laboratory, Livermore, CA, 1984), p. 203.
[14]D. J. Johnson, J. P. Quintenz, and M. A. Sweeney, J. Appl. Phys. **57**, 794 (1985).
[15]Y. Maron, M. Sarfaty, L. Perelmutter, O. Zahavi, M. E. Foord, and E. Sarid (unpublished).
[16]Y. Maron, E. Sarid, E. Nahshoni, and O. Zahavi, following paper, Phys. Rev. A **39**, 5856 (1989).
[17]S. I. Braginskii, in *Reviews of Plasma Physics,* edited by M. A. Leontovich (Consultants Bureau, New York, 1965), Vol. 1, p. 205.
[18]R. C. Davidson and N. T. Gladd, Phys. Fluids **18**, 1327 (1975).
[19]R. C. Davidson, Phys. Fluids **21**, 1375 (1978).
[20]Y. Maron, M. D. Coleman, D. A. Hammer, and H. S. Peng, J. Appl. Phys. **61**, 4781 (1987).
[21]H. R. Griem, *Spectral Line Broadening* (Academic, New York, 1974).
[22]N. Konjević (private communication).
[23]M. S. Dimitrijević and N. Konjević, J. Quant. Spectrosc. Radiat. Transfer **24**, 451 (1980).
[24]M. A. El-Farra and T. P. Hughes, J. Quant. Spectrosc. Radiat. Transfer **30**, 335 (1983).
[25]W. L. Wiese, D. E. Kelleher, and V. Helbig, Phys. Rev. A **11**, 1854 (1975).
[26]H. Ehrich and D. E. Kelleher, Phys. Rev. A **21**, 319 (1980); D. H. Oza, R. L. Greene, and D. E. Kelleher, Phys. Rev. A **37**, 531 (1988).
[27]E. Sarid, L. Perelmutter, M. Markovits, and Y. Maron, Bull. Am. Phys. Soc. **31**, 1509 (1986).
[28]C. Litwin and Y. Maron, Phys. Fluids B **1**, 670 (1989).
[29]D. S. Prono, H. Ishizuka, E. P. Lee, B. W. Stallard, and W. C. Turner, J. Appl. Phys. **52**, 3004 (1981).
[30]J. Halbritter, IEEE Trans. Electron. Ins. **EI-18**, 253 (1983); J. Appl. Phys. **53**, 6475 (1982).
[31]I. G. Newsham, J. V. Hogue, and D. R. Sandstrom, J. Vac. Sci. Technol. **9**, 596 (1972).
[32]R. Clampitt, Polymer **10**, 721 (1969).
[33]J. H. Leck and B. P. Stimpson, J. Vac. Sci. Technol. **9**, 293 (1972).
[34]E. A. Litvinov, G. A. Mesyats, and D. I. Proskurovskii, Usp. Fiz. Nauk **139**, 265 (1983) [Sov. Phys.—Usp. **26**, 138 (1983)].
[35]P. A. Redhead, J. P. Hobson, and E. V. Kornelsen, *The Physical Basis of Ultrahigh Vacuum* (Chapman and Hall, London, 1968).
[36]T. E. Madey and J. T. Yates, Jr., J. Vac. Sci. Technol. **8**, 525 (1971).
[37]G. M. McCraken and D. E. Post, Nucl. Fusion **19**, 889 (1979); U. Daybelge and B. Bien, Phys. Fluids **24**, 1190 (1981); K. Theilhaber and C. K. Birdsall (unpublished).
[38]See, for example, E. W. Gray, J. Appl. Phys. **58**, 132 (1985), and references therein.
[39]R. A. Gerber, K. W. Bieg, E. J. T. Burns, P. L. Dreike, J. E. Maenchen, T. A. Mehlhorn, J. N. Olsen, A. L. Pregenzer, J.

K. Rice, M. A. Sweeney, G. C. Tisone, and J. R. Woodworth, 1985 Particle Accelerator Conference, Vancouver, B.C., 1985 (unpublished).
[40]N. A. Krall and A. W. Trivelpiece, *Principles of Plasma Physics* (McGraw-Hill, New York, 1973).
[41]Y. Chen and C. K. Birdsal, Phys. Fluids **26**, 180 (1983).
[42]B. B. Kadomstev, *Plasma Turbulence* (Academic, New York, 1965), Chaps. I and IV.
[43]P. C. Liewer and N. A. Krall, Phys. Fluids **16**, 1953 (1973).
[44]P. A. Miller, J. W. Poukey, and T. P. Wright, Phys. Rev. Lett. **35**, 940 (1975).